Silicon waveguides for creating quantum-correlated photon pairs

Q. Lin and Govind P. Agrawal

Institute of Optics, University of Rochester, Rochester, New York 14627

Received May 16, 2006; accepted August 2, 2002;
posted August 17, 2006 (Doc. ID 71056); published October 11, 2006

We propose to use four-wave mixing inside silicon waveguides for generating quantum-correlated photon pairs in a single spatial mode. Such silicon-based photon sources not only exhibit high pair correlation but also have high spectral brightness. As the proposed scheme is based on mature silicon technology, it has the potential of becoming a cost-effective platform for on-chip quantum information processing applications.

OCIS codes: 190.4380, 130.4310, 270.0270, 270.5290.

Quantum-correlated photon pairs are conventionally generated by spontaneous parametric downconversion in bulk crystals.[1] Recently it was shown that four-wave mixing (FWM) in optical fibers can generate such photon pairs with much higher brightness.[2–5] However, this scheme suffers from the broadband spontaneous Raman scattering (SpRS) that inevitably accompanies FWM in silica fibers.[6] FWM can occur in any material with a third-order nonlinearity. In particular, silicon exhibits a Kerr nonlinearity more than 200 times larger than fused silica. Moreover, its relatively large refractive index allows silicon waveguides to confine light within an area less than one-fiftieth of that of standard silica fibers. As a result, nonlinear effects are enhanced by more than a factor of 10,000, a feature that enables FWM within a silicon waveguide only a few centimeters long.[7,8] In this Letter we propose to use FWM inside silicon waveguides for generating correlated photon pairs in a single spatial mode with both high brightness and high quality.

We focus on the FWM induced by a single cw pump launched at ω_p, where the three waves are copolarized in either TM or TE mode inside a waveguide conventionally fabricated along the $[\bar{1}10]$ direction on the (001) surface[7,8] (see the inset in Fig. 1). Photon energy conservation requires $2\omega_p=\omega_s+\omega_i$, where ω_s and ω_i are frequencies of signal and idler photons, respectively. The pump can be treated classically and is assumed to remain undepleted because it is much more intense than the signal and idler. By use of the third-order nonlinear polarization of silicon, the pump wave is found to satisfy[9]

$$\frac{\partial A_p}{\partial z}=i[k_p+\gamma(0)I_p]A_p-\frac{1}{2}[\alpha_{lp}+\alpha_{fp}(z)]A_p, \qquad (1)$$

where $k_p\equiv k(\omega_p)$ is the propagation constant at ω_p. The pump field amplitude A_p is normalized such that $I_p(z)=|A_p(z)|^2$ represents its optical intensity.

The signal and idler are treated quantum mechanically to describe photon-pair creation. In the Heisenberg picture, the field operator at ω_s satisfies[6,9,10]

$$\begin{aligned}\frac{\partial\hat{A}(z,\omega_s)}{\partial z}&=ik_s\hat{A}(z,\omega_s)-\frac{1}{2}[\alpha_{ls}+\alpha_{fs}(z)]\hat{A}(z,\omega_s)\\&+i[\gamma(0)+\gamma(\Omega_s)]I_p\hat{A}(z,\omega_s)\\&+i\gamma(\Omega_s)A_p^2\hat{A}^{\dagger}(z,\omega_i)+\hat{m}_l(z,\omega_s)+\hat{m}_f(z,\omega_s)\\&+\hat{m}_T(z,\omega_s)A_p+i\hat{m}_R(z,\Omega_s)A_p, \qquad (2)\end{aligned}$$

where $\Omega_s=\omega_s-\omega_p$. The idler equation can be obtained by exchanging the subscripts s and i. The field operators are normalized to satisfy $[\hat{A}(z,\omega_\mu),\hat{A}^{\dagger}(z,\omega_\nu)]=2\pi\delta(\omega_\mu-\omega_\nu)$.

In the preceding equations, $\alpha_{lj}\equiv\alpha_l(\omega_j)$ $(j=p,s,i)$ represents linear scattering loss, assumed to be the same for all three waves, $\alpha_{lj}\approx\alpha_{lp}$. As optical fields outside can also be scattered into the waveguide, scattering noises are introduced into the signal and idler waves[11]; they are represented by $\hat{m}_l$.

Free-carrier absorption (FCA) is included through $\alpha_{fj}(z)\equiv\alpha_f(z,\omega_j)=\sigma(\omega_j)N_{eh}(z)$, where σ is the FCA coefficient and $N_{eh}(z)=\tau_0\beta_T I_p^2(z)/(2\hbar\omega_p)$ is the carrier density created through two-photon absorption (TPA) induced by a cw pump.[7–9] β_T is the TPA coefficient,

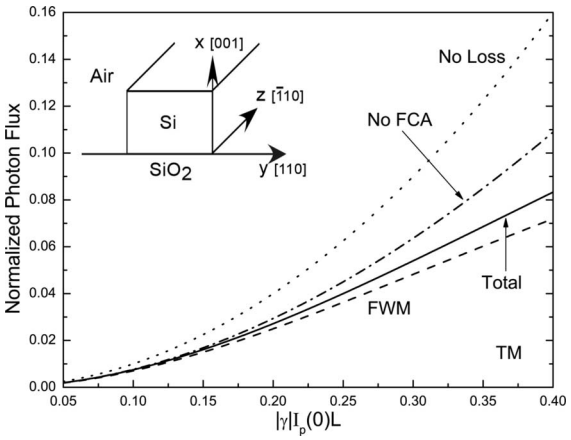

Fig. 1. Normalized photon flux $F_s/\Delta\nu_s$ for the TM mode as a function of input pump intensity for $\beta_T=0.45$ cm/GW, $n_2=6\times10^{-5}$ cm^2/GW, and $\sigma(\omega_p)=1.45\times10^{-17}$ cm^2 at $\lambda_p=1.55$ μm (Ref. 9); other parameters are given in the text. Inset, waveguide geometry.

0146-9592/06/213140-3/$15.00

and τ_0 is the carrier lifetime. As $\alpha_f(z,\omega_j) \propto 1/\omega_j^2$,[7–9] it changes only by about 10% even for a frequency variation of 10 THz. To simplify the following analysis, we use $\alpha_{fj}(z) \approx \alpha_{fp}(z)$. Coupling of free carriers to the background photon reservoir introduces FCA noise, which is represented by $\hat{m}_f$.

The nonlinear parameter $\gamma(\Omega_s) = \gamma_e + \gamma_R(\Omega_s)$ consists of the contributions from both bound electrons (γ_e) and optical phonons (γ_R). The electronic response $\gamma_e = \gamma_0 + i\beta_T/2$ includes both Kerr nonlinearity ($\gamma_0 = n_2\omega_p/c$) and TPA.[9] As the TPA process can simultaneously absorb a pump photon and a signal (or idler) photon, it imposes losses on the signal and idler and thus introduces TPA noise,[10] represented by $\hat{m}_T$.

Resonant interaction with optical phonons introduces Raman scattering, whose strength is given by Raman gain/loss coefficient $g_R(\Omega_s) \equiv 2\,\mathrm{Im}[\gamma_R(\Omega_s)]$. Because of the intrinsic symmetry of silicon, Raman scattering is absent for the TM mode ($\gamma_R = 0$) for the waveguide geometry of Fig. 1, but for the TE mode, it exhibits a narrow peak (103 GHz FWHM) located 15.6 THz away from the pump. Coupling to the phonon reservoir introduces SpRS[12] represented by $\hat{m}_R$.

The four noise operators obey a commutation relation of the form[6,9–11]

$$[\hat{m}_j(z_1,\omega_\mu), \hat{m}_j^\dagger(z_2,\omega_v)] = 2\pi D_j \delta(\omega_\mu - \omega_v)\delta(z_1 - z_2), \quad (3)$$

where D_j ($j = l, f, T, R$) stands for $\alpha_l(\omega_\mu)$, $\alpha_f(z_1,\omega_\mu)$, $2\beta_T$, and $g_R(\Omega_\mu)$ for the four noise sources, respectively. In the case of SpRS, photon frequency ω in Eq. (3) is replaced by phonon frequency $\Omega = \omega - \omega_p$, as $\hat{m}_R(z,\Omega)$ represents the noise operator for the phonon reservoir.[6,11]

The electronic response of nonlinearity is nearly instantaneous. It provides ultrabroadband FWM[8] and thus enables simultaneous creation of signal–idler photon pairs. FWM is a coherent process, requiring phase matching among the interacting waves. We are primarily interested in the spectral region where the phase-matching condition is satisfied and the FWM efficiency is maximum. Thus, as is usually done in practice,[2–5] we assume that two narrowband filters, with transmission functions of $H_\mu(\omega - \omega'_\mu)$ centered at ω'_μ ($\mu = s, i$), are placed at the waveguide output to select the signal and idler frequencies at the center of the phase-matched window with $\omega'_s + \omega'_i = 2\omega_p$. Consequently, the output fields become $\hat{A}_\mu(\tau) = \int H_\mu(\omega - \omega'_\mu)\hat{A}(L,\omega)e^{-i\omega\tau}\mathrm{d}\omega/2\pi$, where we designate the signal as the anti-Stokes with $\omega'_s > \omega_p$.

For correlated photon-pair generation, the pump intensity is kept relatively low [$|\gamma| I_p(0)L \ll 1$] to prevent stimulated scattering. As Eq. (2) is linear, following Ref. 6, we can find the solution $\hat{A}(L,\omega)$. Using it and averaging over the vacuum input and background photon and phonon reservoirs,[6,10,12] we obtain the signal/idler photon flux, $F_\mu \equiv \langle \hat{A}_\mu^\dagger(\tau)\hat{A}_\mu(\tau)\rangle$. Further analysis can be simplified considerably if we note that all loss mechanisms introduce noise through coupling to a thermal photon reservoir with a population of $n_T = [\exp(\hbar\omega_\mu/k_BT) - 1]^{-1}$. As the photon energy $\hbar\omega_\mu$ ($\sim$0.8 eV) is generally much larger than the thermal energy $k_BT \approx 26$ meV at room temperature ($T = 300$ K), $n_T \approx 0$, and the photon reservoir can be treated as vacuum. The situation is different for SpRS, which is coupled to a phonon reservoir[12] with a population of $n_{th}(\Omega) = [\exp(\hbar|\Omega|/k_BT) - 1]^{-1}$. As the phonon energy ($\hbar|\Omega| \approx 65$ meV) at the Brillouin-zone center is comparable with k_BT, SpRS is not negligible. Under these considerations and assuming $|\gamma| I_p(0)L \ll 1$, the photon flux is given by

$$F_\mu = \Delta\nu_\mu \left[|\gamma|^2 \eta(0,L)\mathcal{I}^2(0) + |g_R|\mathcal{N}_\mu \int_0^L I_p(z)\,\eta(z,L)\mathrm{d}z + |\gamma|^2 \int_0^L \alpha(z)\,\eta(z,L)\mathcal{I}^2(z)\mathrm{d}z \right], \quad (4)$$

where $\Delta\nu_\mu$ is the filter bandwidth, $\mathcal{N}_s = n_{th}$ but $\mathcal{N}_i = n_{th} + 1$; n_{th}, γ, and g_R are all calculated at phonon frequency $\Omega_0 = \omega'_s - \omega_p$.[6] Further, $\alpha(z) \equiv \alpha_{lp} + \alpha_{fp}(z) + 2\beta_T I_p(z)$ is the total loss, $\eta(z,L) = \exp\{-\int_z^L \alpha(z')\mathrm{d}z'\}$, and $\mathcal{I}(z) = \int_z^L I_p(z')\mathrm{d}z'$.

Equation (4) shows that the generated photon flux consists of three sources. The first term is due to FWM and is the source of correlated photon pairs. The second term is due to SpRS, which generates more idler photons than the signal photons. It vanishes for the TM mode and becomes large for the TE mode only when $\Omega_0/2\pi$ is close to 15.6 THz. The last term represents noise photons generated through FWM seeded by loss-induced noise. It is relatively small when the pump intensity is low ($|\gamma| I_p(0)L \ll 1$), and its magnitude is nearly the same for both the signal and the idler.

Figure 1 shows the growth of the normalized photon flux $F_s/\Delta\nu_s$ for the TM mode of a 3 cm waveguide with a linear loss of 0.2 dB/cm and a carrier lifetime of 1 ns (solid curve). In the ideal case without any loss, $F_s = \Delta\nu_s|\gamma I_p(0)L|^2$, and the flux grows quadratically with pump intensity (dotted curve). Losses reduce the flux because they attenuate the pump and absorb signal/idler photons. In general, linear scattering loss dominates (dashed-dotted curve) and reduces the photon flux by 24%. Our analysis shows that both TPA and FCA only play a minor role if $|\gamma| I_p(0)L \leq 0.2$. For example, their magnitudes are less than 0.1 dB/cm for $|\gamma| I_p(0)L = 0.2$. The dashed curve in Fig. 1 shows the photon flux created by FWM alone [the first term of Eq. (4)]. Its comparison with the solid curve shows that noise photon flux is $<8\%$ for $|\gamma| I_p(0)L < 0.2$, indicating a relatively high quality of created photon pairs.

The quality of photon pairs can be quantified with the quantum correlation defined as $\rho(\tau) = P_{si}(\tau)/(F_sF_i) - 1$, where $P_{si}(t,\tau) = \langle \hat{A}_i^\dagger(t)\hat{A}_s^\dagger(t+\tau)\hat{A}_s(t+\tau)\hat{A}_i(t)\rangle$ is the biphoton probability of a signal–idler pair. When $|\gamma| I_p(0)L \ll 1$, the pair correlation is given by

$$\rho(\tau) = C_f \left| i\gamma\eta(0,L)\mathcal{I}(0) - |g_R| n_{th} \int_0^L I_p(z)\,\eta(z,L)\mathrm{d}z + i\gamma \int_0^L \alpha(z)\,\eta(z,L)\mathcal{I}(z)\mathrm{d}z \right|^2, \quad (5)$$

where $C_f(\tau) \equiv |\varphi(\tau)|^2 \Delta\nu_s \Delta\nu_i/(F_s F_i)$ depends on the signal and idler filters through $\varphi(\tau)$ (Ref. 6); $|\varphi(0)|^2 = 1$ for two identical filters.

Equations (4) and (5) are quite general, as they include the effects of all noise sources. Since SpRS is either absent (TM mode) or occurs only over a narrow bandwidth near $\Omega_0/2\pi \approx 15.6$ THz (TE mode), we can neglect it in most cases of interest. Equation (5) then reduces to

$$\rho(\tau) = \frac{|\varphi(\tau)|^2}{|\gamma|^2} \left[\frac{\mathcal{I}(0) + \int_0^L \alpha(z)\,\eta^{-1}(0,z)\mathcal{I}(z)\mathrm{d}z}{\mathcal{I}^2(0) + \int_0^L \alpha(z)\,\eta^{-1}(0,z)\mathcal{I}^2(z)\mathrm{d}z} \right]^2. \quad (6)$$

It reduces further to $\rho(\tau) = |\varphi(\tau)|^2/|\gamma I_p(0)L|^2$ for a pure FWM process without any loss.

Figure 2 shows $\rho(0)$. The correlation decreases with increased pump intensity because of an enhanced probability of multiphoton generation. Nevertheless, silicon-based photon production exhibits relatively high values of $\rho(0)$. It is 490 when $|\gamma| I_p(0)L = 0.05$ and varies from 126 to 34 when $|\gamma| I_p(0)L$ changes from 0.1 to 0.2. The pair correlation is about 11 even when $|\gamma| I_p(0)L$ becomes as large as 0.4. These values are among the highest values available from fiber-based photon sources for a given photon-flux level.[2–6] They are available at any photon frequency below the silicon absorption edge of 1.1 eV.

Silicon-based FWM is very efficient for photon-pair generation. Figure 2 shows the spectral brightness defined as $F_s/[\Delta\nu_s I_p(0) a_{\mathrm{eff}}]$, assuming an effective area of $a_{\mathrm{eff}} = 0.4\ \mu\mathrm{m}^2$.[9] Only the purely FWM-generated photon flux [first term in Eq. (4)] is plotted, as it provides the true coincidence counting rate in practice. As expected, spectral brightness grows linearly with pump intensity; a slight saturation at high pump levels is due to FCA (it can be reduced by using a pulsed pump[9]). For typical values of $|\gamma| I_p(0)L \sim 0.1$–$0.2$ for which $\rho(0)$ exceeds 30, the spectral brightness is in the range of 1.3×10^5 to 2.3×10^5 pairs/s/GHz/mW. These values are comparable with the highest values available in optical fibers[2–5] but without any effect of SpRS. They are also comparable with those available in periodically poled $LiNbO_3$ waveguides[12,13] but without any temperature control requirement and with a much simpler fabrication platform based on silicon technology.

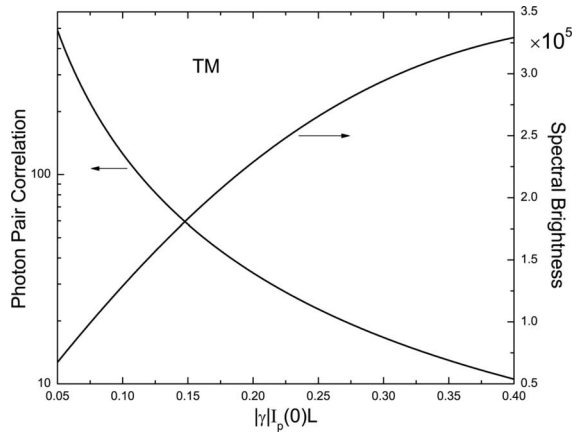

Fig. 2. Photon-pair correlation $\rho(0)$ and spectral brightness under the conditions of Fig. 1. The spectral brightness has the units pairs/s/GHz/mW.

Although previous discussion focuses on the TM mode, our results apply to the TE mode as well. Only when $\Omega_0/2\pi \approx 15.6$ THz does strong Raman scattering enhance FWM.[7,9] Although this increases spectral brightness considerably, SpRS dominates over FWM in photon production, especially for the idler at the Stokes, leading to dramatic degradation in pair correlation.[6] Such a Raman-assisted scheme is not suitable for photon-pair generation. Note that SpRS can be eleminated even for the TE mode by fabricating the waveguide along the [010] direction.

In conclusion, we have presented a theory to quantify the quality of photon pairs generated by FWM in silicon waveguides. We show that photon pairs not only exhibit high correlation qualities because of absence of SpRS but also have a high spectral brightness that is comparable with any other photon-pair sources. As the proposed scheme is based on mature silicon technology, we believe it would become an efficient but cost-effective platform for future on-chip quantum information processing.

The authors thank F. Yaman and J. Zhang for helpful discussions. This work is supported by the National Science Foundation under grants ECS-0320816 and ECS-0334982.

References

1. P. G. Kwiat, E. Waks, A. G. White, I. Appelbaum, and P. H. Eberhard, Phys. Rev. A **60**, R773 (1999).
2. X. Li, J. Chen, P. Voss, J. Sharping, and P. Kumar, Opt. Express **12**, 3737 (2004).
3. H. Takesue and K. Inoue, Phys. Rev. A **72**, 041804(R) (2005).
4. J. Fan, A. Migdall, and L. J. Wang, Opt. Lett. **30**, 3368 (2005).
5. J. Fulconis, O. Alibart, W. J. Wadsworth, P. St. J. Russell, and J. G. Rarity, Opt. Express **13**, 7572 (2005).
6. Q. Lin, F. Yaman, and G. P. Agrawal, Opt. Lett. **31**, 1286 (2006).
7. V. Raghunathan, R. Claps, D. Dimitropoulos, and B. Jalali, J. Lightwave Technol. **23**, 2094 (2005).
8. H. Rong, Y. Kuo, A. Liu, M. Paniccia, and O. Cohen, Opt. Express **14**, 1182 (2006).
9. Q. Lin, J. Zhang, P. M. Fauchet, and G. P. Agrawal, Opt. Express **14**, 4786 (2006), and references therein.
10. S. Ho, X. Zhang, and M. K. Udo, J. Opt. Soc. Am. B **12**, 1537 (1995).
11. H. A. Haus, *Electromagnetic Noise and Quantum Optical Measurements* (Springer, 2000), Chap. 6.
12. L. Boivin, F. X. Kärtner, and H. A. Haus, Phys. Rev. Lett. **73**, 240 (1994).
13. S. Tanzilli, W. Tittel, H. De Riedmatten, H. Zbinden, P. Baldi, M. De Micheli, D. B. Ostrowsky, and N. Gisin, Eur. Phys. J. D **18**, 155 (2002).
14. F. König, E. J. Mason, F. N. C. Wong, and M. A. Albota, Phys. Rev. A **71**, 033805 (2005).